

This paper was recommended for publication in revised form by Co-Editor Burcu Acunaş

EXPERIMENTAL AND 1-D MODEL ANALYSIS OF WANKEL ENGINE AT PART LOAD

Ö.Cihan¹, M.Aydın², O.A.Kutlar³

ABSTRACT

Nowadays, Wankel type rotary engines are being studied which find use area in various fields due to vibration, lightness and power obtained from unit volume. In this study; A Wankel engine is used 13B-MSP (Multi Side Port) single-rotor, 4-stroke and port fuel injection. Experimentals are used 2 bar and 3 bar under partial load and 1500, 2000, 2500, 3000, 4000 and 5000 rpm at engine speeds. Experiments are carried out in a stoichiometric mixture. In addition, under the same conditions, the results obtained by analyzing in the AVL Boost program are compared with the experiment results in terms of specific fuel consumption and exhaust emissions. It was determined that the developed model overlaps with the experimental results. It is also seen that specific fuel consumption and exhaust emissions of Wankel engine at new working conditions can be achieved without new experiment via using this model.

INTRODUCTION

Wankel engines are rotary engine based on four stroke working principle. These engines differ in terms of working principle from reciprocating engines. The engine has a rotor and eccentric shaft as moving parts. There are no valve arrangements like reciprocating engines in intake and exhaust strokes. The intake and exhaust process is carried out by the ports on the housing or side housings. The opening and closing times of the ports limit the side face by the movement of the rotor. Charge change is provided through ports. At the same time, the port geometry determines the advance. It also has a simple structure as there is no crank and connecting rod mechanism like reciprocating engines. The rotor in the Wankel motor is responsible for the piston and connecting rod mechanism in linearly moving piston engines. Also, the rotor transmits the power transmission directly to the output shaft, providing rotational motion, thanks to the pressure generated by the burning gases. Wankel engines have the ability to take off at high speeds compared to reciprocating engines, since there is no crank-connecting rod mechanism and no valve assembly.

As can be seen in Figure 1, one revolution of the rotor is completed by rotating the eccentric shaft three revolutions in the Wankel engines. Here, the eccentric shaft is getting a work every revolution. During engine operation, instead of just moving the crankshaft up and down (180 degrees), the eccentric shaft rotates 270 degrees to provide more power [1].

If we look at the advantages of Wankel engines; it can be listed as being lightweight because it is made up of fewer parts, it can operate smoothly because it has less space, less reciprocating masses like pistons and connecting rods, lower NO_x emission values and more power than piston engine with the same weight ratio. Wankel engines are preferred because of their advantages in the aviation sector, especially in unmanned aerial vehicles, due to the low power density of the weight [2-6]. Today, the most intensive work on the Wankel engine is carried out by the Mazda company [7].

In this study, Modeling with the AVL Boost program is compared with the experimental study at partial loads. The RX8 is the Mazda 13B MSP engine (1300 cc) type. No work on modeling Wankel engine with this program has been found in the literature. In this study, the engine is operated stoichiometric mixture at partial

loads (2 and 3 bar mean effective pressure), and at different engine speeds (1500, 2000, 2500, 3000, 4000 and 5000 rpm). Then the parameters obtained in the Boost program are compared with the experimental data in terms of specific fuel consumption and exhaust emissions. The results obtained in the Boost program by a one-dimensional thermodynamic model is found to be close to the experimental results.

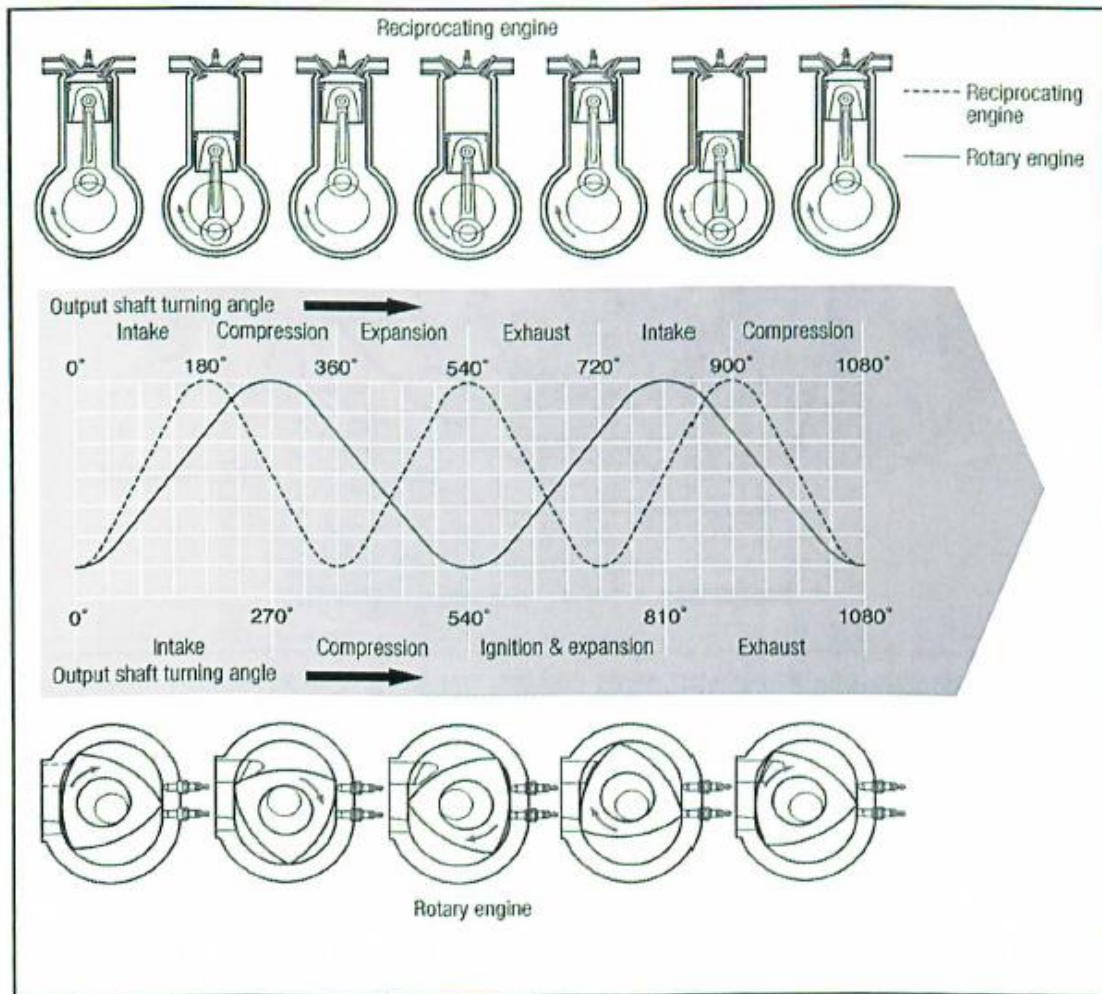


Figure 1. Comparison of reciprocating engine and Wankel engine in terms of working principle [1].

EXPERIMENTAL SETUP

The Mazda 13B MSP (Multi Side Port) is used as a single rotor motor [1]. The engine is originally a two rotor and all parts such as intake, exhaust, lubrication-cooling system, eccentric shaft are manufactured and turned into single rotor test motor. A single-rotor Wankel research engine is connected to the Schenck brand 70 kW power unit, the W70 model electromagnetic brake. The strength of the dynamometer is measured by the load cell. The moment sensitivity of the load sensor is $\pm 0.02\%$. After the motor is connected, the calibration of the dynamometer is renewed at regular intervals. On the other hand, the engine water conditioner unit with a capacity of 90 kW in the engine test room. The unit consists of the fuel consumption measurement system (AVL 733S) and the fuel conditioning unit (AVL 753C). The device operates according to the gravimetric measurement principle and fuel line pressure is set to a value of 4 bar for the fuel temperature of 25°C in the 13B-MSP Wankel engine. Bosch BEA350 garage exhaust gas analyzer and HORIBA Mexa 7500 exhaust gas analyzer are used for measurement of exhaust emissions. Emission devices can measure CO , CO_2 , O_2 , HC , NO , CH_4 and λ (lambda) values. There is an engine control unit which can arrange the ignition and injection timing. Maintenance and calibration of all the devices are carried out in the laboratory. Differences in the results of the measurements made remained below 5% at different times. The Wankel engine experiment room is schematically shown in Figure 2.

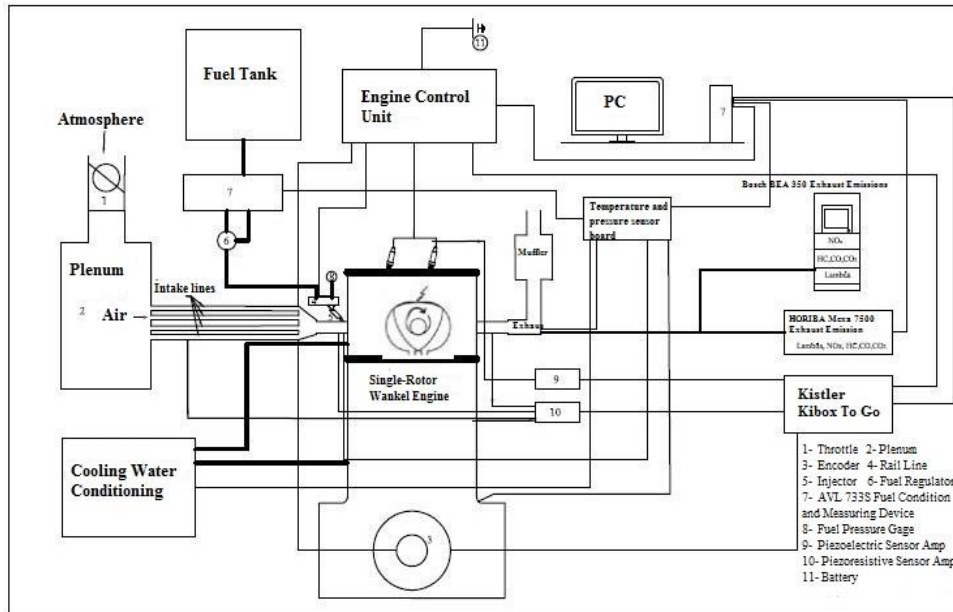


Figure 2. Wankel engine experimental setup.

Experiments are carried out stoichiometric mixture ($\lambda = 1$) and different engine speeds (1500, 2000, 2500, 3000, 4000 and 5000 rpm) at partial load conditions (2 and 3 bar). The opening and closing times of the intake and exhaust ports of the engine are listed in Table 1 and the geometric characteristics of the engine are given in Table 2.

Table 1. Intake and exhaust open-close timings and the other specifications [7].

RENESIS High Power Engine				
Parameters	Port Timing			
	Primary	Secondary	Auxiliary	Exhaust
I.O (ATDC)	3°	12°	38°	-
I.C (ABDC)	65°	36°	80°	-
E.O (BBDC)	-	-	-	50°
E.C (BTDC)	-	-	-	3°
Type	Side Intake	Side Intake	Side Intake	Side Exhaust

Table 2. Geometric data related to the 13B MSP Wankel engine.

Quantity	Value
R (Length center-corner of the rotor)	105 [mm]
e (Eccentricity)	15 [mm]
b (The width of rotor)	80 [mm]
L (Length of the rotor)	180 [mm]
ϵ (Compression ratio)	10
Displacement	654x2 [cc]

NUMERICAL MODEL

Primary intake port at lower engine speed, primary and secondary intake ports at medium engine speed, primary, secondary and auxiliary intake ports at higher engine speed are used to obtain effective torque in double rotary piston 13B MSP Wankel engine. There are two secondary (S1, S2) and two auxiliaries (A1, A2) intake ports in this research engine, which is converted to single rotary piston engine for experiments. In this study, due to the operating under partial load, only secondary suction port was used. Two secondary (S1, S2) intake ports were used at 4000 rpm and higher engine speeds while only one secondary intake port was used up to 4000 rpm engine speed in experimental study. So a numerical model was created in AVL BOOST software by considering these situations.

Specific fuel consumption, HC and NO_x emissions are obtained at determined engine speeds at part loads. In this created model, double-Wiebe function for combustion, Woschni for heat transfer, extended Zeldovich for NO_x formation and the model credited to literature by Lavoie and Blumberg[8] for HC emissions were used. The model created in BOOST software is given in Figure 3.

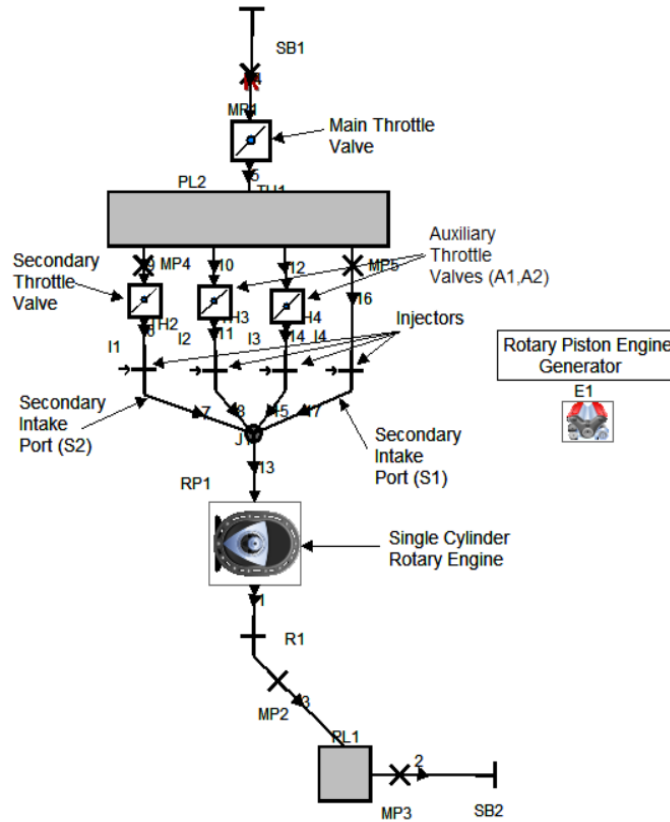


Figure 3. BOOST model for one rotary piston Wankel engine.

In the AVL BOOST software, some empirical expressions and equations are used while analysing exhaust emissions. NO_x emissions, one of the pollutant emissions, were calculated by implementing the six-reaction Zeldovich mechanism used by Pattas and Haefner in their work [9]. Arrhenius coefficients of this reaction mechanism are taken from literature [10]. The expression giving NO_x formation is given in Equation 1.

$$r_{NO} = C_{PostProcMult} * C_{KineticMult} * 20 * \left(1 - \left[\frac{C_{NO,act}}{C_{NO,eq}} \frac{1}{C_{KineticMult}} \right]^2 \right) * \left(\frac{r_1 * (r_2 + r_3) * C_{NO,eq} * C_{KineticMult}}{C_{NO,eq} * C_{KineticMult} * (r_2 + r_3) + C_{NO,act} * r_1} + \frac{r_2 * (r_5 + r_6)}{r_5 + r_6 + r_4} \right) \quad (1)$$

In equation 1, r_i is the elemental reaction rates of the Zeldovich mechanism, $C_{NO,act}$ is the instantaneous molar density of NO molecules, $C_{NO,equ}$ the molar density at equilibrium and $C_{kineticMult}$ is kinetic multiplication which must be calibrated with experimental results [9, 11]. The kinetic multiplier used in this work was optimised with Levenberg- Marquardt method and the expression of kinetic multiplier depending on engine speed and load factor was given in Equation 2.

$$C_{kineticMult} = a * e^{n_i} * C_{AEPF,i} + b * e^{C_{AEPF,i}} * n_i + c * C_{AEPF,i} * n_i + d * C_{AEPF,i} + e * n_i \quad (2)$$

The n_i expresses one thousandth of the number of rotations, C_{AEPF} is the load factor and i is the load case index. Equation coefficients and load factors obtained according to the Levenberg-Marquardt optimization method are given in Table 3.

Table 3. Coefficients of kinetic multiplier for NO_x emissions.

Load	A	b	c	d	e	C_{AEPF}
2 bar	-0.02283	6.755	-5.229	2.338	-6.997	0.2771
3 bar	-0.00166	-0.1739	0.6846	1.446	0.02226	0.9173

On the other hand, to model the HC emission, which is another exhaust gas emission, some numerical coefficients and equations consist of O₂ and HC molar densities were used [8, 12, 13]. The expression of HC oxidation is given in Equation 3.

$$\frac{d[HC]}{dt} = F_{O_x} * A_{O_x} * e^{\frac{T_{O_x}}{T}} * C_{HC}^a * C_{O_2}^b \quad (3)$$

C_i is molar concentrations of HC and O₂ [kmol/m³], F_{O_x} is kinetic multiplier for HC oxidation [-] and it must be calibrated with experimental results [8, 12]. T_{O_x} is the activation temperature and the value is 18790.0 K and A_{O_x} is frequency factor, which is taken as 7.7 e12 [m³/kmole/s] [8]. The numbers a and b in the equation can be taken as 1 for the petrol engine [10]. F_{O_x} , kinetic multiplier, is expressed by the curve fitting method as in Equation 4.

$$F_{O_x} = \alpha * e^{\beta * n} \quad (4)$$

In this equation n is engine speed and the coefficients of the equation calibrated according to the experimental data are given in Table 4 for α and β constants. And to express HC emissions as ppm Equation 5 is used.

Table 4. Coefficients of kinetic multiplier for HC emissions.

Load	α	β
2 bar	0.0006	0.0005
3 bar	0.0003	0.0006

$$HC_{i+1} = \frac{\left([HC]_i - \frac{d[HC]}{dt} * dt\right) * R_u * P * 1000}{T} * 10^4 \quad (5)$$

i index given in Equation 5 represent the number of steps in eccentric shaft angle and the HC emissions remaining in the combustion chamber in the time step $i+1$ is calculated depending on cylinder pressure [kPa], cylinder temperature [K] and ideal gas constant [kJ/kmolK].

RESULTS

Cylinder pressure of the created Wankel engine model in BOOST software was verified by experimental cylinder pressure at 1500, 2000, 2500, 3000 and 4000 rpm engine speeds at part load conditions. But at 5000 rpm engine speed, even cylinder pressure in compression stroke and maximum cylinder pressure were reached, cylinder pressure in combustion stroke was not similar with experimental results.

The NO_x emissions obtained with the numerical model and experimental results at all engine speeds for partial loads are given in Figure 4. It can be easily seen that the NO_x emission values obtained by numerical model under 2 bar mean effective pressure are in the same trend as the experimental results. However, it was observed that the difference between the model and the test results increased with increasing load (3 bar) at increasing engine speeds. The reason for this is that the kinetic factor obtained by the Levenberg-Marquardt method increases more than the experimental result as the load increases. On the other hand, with the increasing of engine load, the amount of charge absorbed into the combustion chamber increases and so it leads to higher combustion temperature. due to the increasing cylinder temperature and combustion efficiency, NO_x emissions increases. But NO_x emissions tend to decrease with respect to rising engine speed, due to the insufficient time for formation of NO_x emissions.

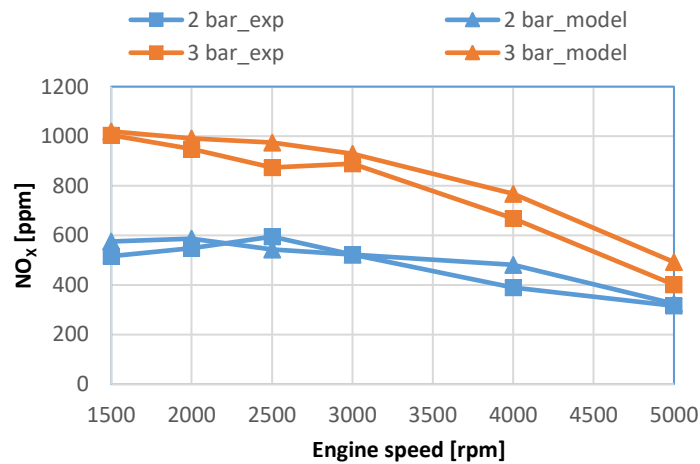


Figure 4. Comparison of NO_x emissions obtained from numerical model and experimental results at different engine speeds at part loads.

Specific fuel consumption values of numerical model are compared with experimental results at all engine speeds at partial loads in Figure 5. Lower specific fuel consumption has been achieved with increased load for all engine speeds. In this study range, it is seen that the results obtained from model are close to the experimental results. But at 5000 rpm engine speed, there is a difference between the experimental results and the model. The reason for this is the increasing of friction between the segments and body which is proportional to the square of engine speed in Wankel engine [14]. On the other hand, despite the increased engine speed, there were no significant changes in the SFC values. This is because specific fuel consumption in partial loads is not significantly affected by engine speed.

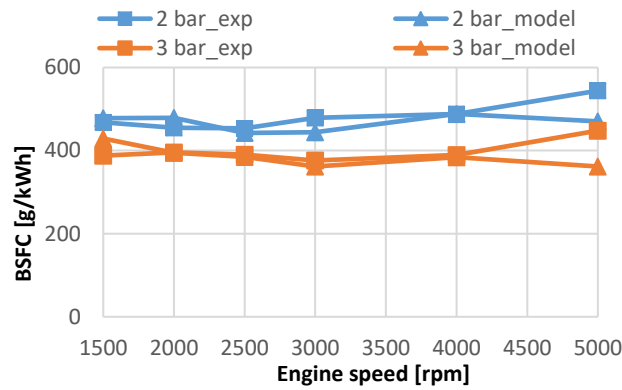


Figure 5. Comparison of specific fuel consumption obtained from numerical model and experimental results at different engine speeds at part loads.

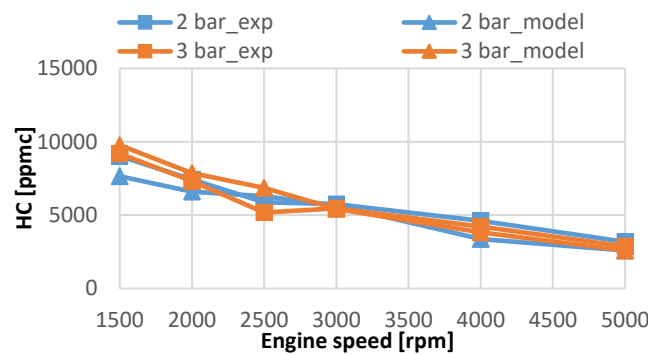


Figure 6. Comparison of HC emissions obtained from numerical model and experimental results at different engine speeds at part loads.

In this studied range, the HC emissions obtained from experimental results and the numerical model are compared in Figure 6. In this model, after the kinetic multiplier was calibrated depending on load and engine speeds, HC emissions close to experimental results were obtained. However, the difference between experiment and model is the most 15 % and it occurred at 1500 and 4000 rpm engine speeds at 2 bar mean effective pressure and 2500 rpm engine speed at 3 bar MEP. The reason for this is that the emissions cannot be modelled according to local conditions and the calibrated kinetic factor is expressed in a one-dimensional equation.

On the other hand, in the entire working conditions, although the changing in the load, there is no difference in HC emissions. But increased engine speed caused to reduction of HC emissions. This is because increased turbulence in the combustion chamber with the increasing engine speed, better mixture formation and improved combustion.

CONCLUSION

Experiments were performed at engine speeds of 1500, 2000, 2500, 3000, 4000 and 5000 rpm at partial loads (2 and 3 bar), after converting the 13B MSP double rotor Wankel engine into a single cylinder test engine. Experiments and simulations were done at stoichiometric condition ($\lambda=1$) at all working range. The specific fuel consumption, HC and NO_x emissions from the experiments results were compared with the model which is generated by actual engine operating conditions with one dimensional BOOST software.

Because BOOST software is a one-dimensional model, there is no possibility to model local temperature and local emission occurrences in the combustion chamber. So it allows to calculate emissions by taking into the account the mean combustion temperatures. Therefore, the kinetic multipliers for emission models were calibrated to load and engine speed. Using the kinetic multiplier curve developed for different engine loads and speeds, the performance and exhaust emission values can be predicted by one-dimensional model in Wankel engine. But in this study, there are some differences between model and experimental results, although the kinetic multiplier was used. The reason for the difference between the exhaust emission results obtained from the model and the results

obtained from the experiment is the difference between the selected kinetic multiplier and the curve determined by the Levenberg-Marquardt method. Therefore, the kinetic multiplier must be developed by creating extended equation which is consist of experimental data about different engine speeds, loads and amount of mixture charge.

At partial loads and different operating engine speeds, there is no significant change in specific fuel consumptions. On the other hand, as engine speed increases for both loads, NO_x emissions decrease due to the time for kinetic reactions decrease. In addition, HC oxidation is accelerated due to increased engine speed and increased turbulence intensity. But the effect of engine load cannot be observed.

NOMENCLATURE

HC	Hydrocarbon
BSFC	Break Specific Fuel Consumption
NO	Nitrogen Oxides
CO	Carbon Monoxides
CO ₂	Carbon Dioxides
O ₂	Oxygen
CH ₄	Methane
ATDC	After Top Dead Center
ABDC	After Bottom Dead Center
BTDC	Before Top Dead Center
BBDC	Before Bottom Dead Center
I.O	Inlet Port Open
I.C	Inlet Port Close
E.O	Exhaust Port Open
E.C	Exhaust Port Close

REFERENCES

- [1] Warner, M. (2009). Street Rotary, USA: Penguin Group.
- [2] Ansdale, R.F. (1968). The Wankel RC Engine, London: W.C.I: Ilife Books Ltd.
- [3] Yamamoto, K. (1971). Rotary Engine, Tokyo, Japan: Sankaido.
- [4] Yamamoto, K. (1981). Rotary Engine, Tokyo, Japan: Sankaido.
- [5] Froede, W. G. (1961). The Nsu-Wankel rotating combustion engine. SAE Paper.
- [6] Wankel, K. (1963). Einteilung der Rotations-Kolbenmaschinen Stuttgart.
- [7] Ohkubo, M., Tashima S., Shimizu, R., Fuse, S. and Ebino, H. (2004).Development technologies of the new rotary engine (RENESES), SAE Paper 2004-01-1790.
- [8] Lavoie, G. A. and Blumberg, B. N. (1980). A fundamental model for predicting combustion, NO_x, and HC emissions of the conventional spark-ignition engines, Combustion Science and Technology, vol. 21, pp. 225-258.
- [9] Pattas, K. and Hafner, G. (1973). Stickoxidbildung bei der ottomotorischen Verbrennung, MTZ, no. 12, pp. 397-404.
- [10] AVL LIST GmbH, AVL BOOST Theory tutorial, BOOST 2013v1.
- [11] Lesnik, L. and Bilus. I. (2016). The effect of rapessed oil biodiesel fuel on combustion performance and the emission formation process within a heavy-duty DI diesel engine. Energy Conversion and Manegement, no. 109, pp. 140-152.
- [12] Schramm, J. and Sorenson, S.C. (1990). A model for Hydrocarbon Emissions from SI Engines, International Fuels and Lubricants Meeting and Exposition, Tulsa, Oklahoma, October 22-25.
- [13] Url-1<<http://nptel.ac.in/courses/112104033/8>>. Date retrieved 10.12.2017.
- [14] BASHUYSEN, R., STUTZENBERGER, H. and VOGT, R. (1982). Unterschiede im Reibungsverhalten zwischen Kreis- und Hubkolbenmotoren von Audi, ATZ Automobiltechnische Zeitschrift, 84(11), 573-576.